Instrumentation for Epidural Anesthesia

King-wei Hor[1], Denis Tran[1], Allaudin Kamani[2], Vickie Lessoway[3], and Robert Rohling[1]

[1] Department of Electrical and Computer Engineering, University of British Columbia, Vancouver, BC, Canada
{kingh, denist, rohling}@ece.ubc.ca
[2] Department of Anesthesia, B. C. Women's Hospital, Vancouver, BC, Canada
[3] Department of Ultrasound, B. C. Women's Hospital, Vancouver, BC, Canada

Abstract. A low-cost, sterilizable and unobtrusive instrumentation device was developed to quantify and study the loss-of-resistance technique in epidural anesthesia. In the porcine study, the rapid fall of the applied force, plunger displacement and fluid pressure, and the oral indication of the anesthesiologists were shown to be consistent with the loss-of-resistance. A model based on fluid leakage was developed to estimate the pressure from the force and displacement measurements, so that the pressure sensor could be omitted in human studies. In both human (in vivo) and porcine (in vitro) subjects, we observed that the ligamentum flavum is less amenable to saline injection than the interspinous ligament.

1 Introduction

Epidural anesthesia (or epidural) is an important and widely accepted analgesia technique in obstetrics to effectively alleviate labor pain. To facilitate the delivery of the local anesthetic, a catheter is inserted through a needle into the epidural space, a narrow space surrounding the dura mater within the spinal column. A widely accepted method known as the loss-of-resistance technique is used to indicate entry of the needle tip into the epidural space, located anterior to the ligamentum flavum. When the needle advances through the supraspinous ligament, interspinous ligament and then the ligamentum flavum, the anesthesiologist continuously feels a high resistance to injection of saline or air. Upon entry into the epidural space, the ease of injection causes the anesthesiologist to feel the loss-of-resistance and needle advancement is then halted.

Like all other obstetric interventions, epidural anesthesia involves risks. Complications can include backache, headache, shivering, hypotension, bladder dysfunction and inadequate pain relief. More rare are the inadvertent dural puncture, fetal distress, neurologic injury, cardiac arrest, allergic shock and maternal death. Although the use of conventional epidurals has increased over a few decades, it continues to have a failure rate in the range of 6–25% [1,2]. One study shows a success rate of 60% after 10 attempts and 84% after 60 attempts [3]. Epidurals are considered more difficult than other regional anesthetic techniques [4]. Although residents can practice on cadavers or simulated tissues

N. Ayache, S. Ourselin, A. Maeder (Eds.): MICCAI 2007, Part II, LNCS 4792, pp. 918–925, 2007.

and ligaments, none provide accurate haptic feedback [5]. Much of the experience is gained by performing the epidural anesthesia on actual human patients but patient risk is involved. Furthermore, the risk of complication is increased due to anatomical variations from patient variability (such as age, height, BMI, ethnicity, etc.).

Improving the learning curve while avoiding patient risks would be beneficial, so there have been attempts to construct epidural simulators [5,6]. These simulators provide force feedback with sub-optimal realism [5] and have not found wide acceptance. This may be due to subtleties and dynamic interactions that exist only while performing the actual epidural on human subjects in vivo.

Anesthesiologists continue to rely on the loss-of-resistance technique as the only feedback mechanism to indicate entry into the epidural space, but the technique is not completely reliable [7]. There are no external physical characteristics of the patient that can provide information of the exact location of the epidural space. Having to solely rely on this technique means the patient is exposed to all its associated risks. Recently, ultrasound is being used in a limited fashion to help visualize the involved anatomy but further scientific evaluation and validation is required [8]. Since the loss-of-resistance is a crucial technique, there is a need for good instrumentation.

Specifically, the first goal is to determine whether the loss-of-resistance can be measured accurately with unobtrusive sensors. Another goal is to determine whether any tissue properties can be derived from the measurements. The overall goal is to gain a deeper understanding of the loss-of-resistance method which may help further research in more accurate simulators and computer models.

To quantifiably detect the loss-of-resistance, the force of the thumb acting on the plunger of the syringe F_a, the displacement of the plunger relative to the barrel D, and the pressure of the saline fluid P were instrumented, as shown in Figure 1. These measured quantities were used to investigate the influence of the tissue type in both laboratory and clinical settings. Ultrasonography was used to validate the loss-of-resistance technique by comparing the depth of the depicted epidural space to the length of the inserted portion of the needle. Consistency of the measured location of the epidural space in the ultrasound image and by the loss-of-resistance technique is essential for furthering fundamental research towards the goal of real-time ultrasound-assisted guidance with sensory feedback.

2 Methods

2.1 Instrumentation

Instrumenting the three physical quantities, F_a, D and P, required three individual sensors. The SLB-25 force sensor (Transducer Techniques, Temecula, CA) was used to measure F_a, the CSPR IP65 displacement sensor (MTS System, Cary, NC) was used to measure D, and the PX302 pressure sensor (Omega Engineering, Stamford, CT) was used to measure P, as illustrated in Figure 1. A custom-built stainless steel harness, fitted to the anesthesiologist's thumb, was used to mount the force sensor. The pressure sensor was connected to a three-way

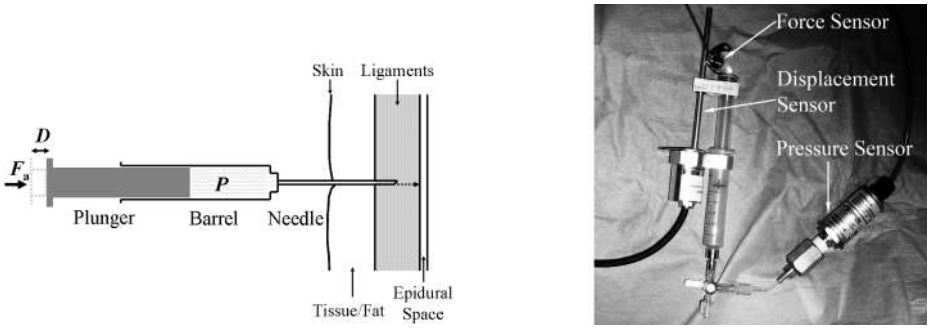

Fig. 1. The loss-of-resistance was instrumented by using three sensors that measured the applied force F_a, the plunger displacement D and the saline fluid pressure P

stopcock that was attached to the needle seat of the syringe. The ring magnet of the magnetostrictive displacement sensor was attached to the plunger and its transducer rod was attached to the barrel by a custom-built stainless steel harness. The ring did not touch the rod, so friction was negligible and allowed the anesthesiologist to retain the full feeling of loss-of-resistance. Glass syringes (JH-0550 Epidural Catheterization Kit, Arrow International, Reading, PA) were used for the studies. The Q8 data acquisition board (Quansar, Markham, ON) was used to capture the sensor signals to a PC at a sampling rate of 0.01 s. For calculations, a moving average filter with an interval size of 0.1 s was used to remove the majority of the noise.

2.2 Modeling

Three models relating the measurement variables were investigated: the static, dynamic and decay model. Each model incorporates different physical and empirical properties to relate the pressure to the force and displacement measurements.

The static model describes a non-dynamic system with no motion or fluid flow. The fundamental relationship describing the pressure $P(t)$ varying over time t of an incompressible static fluid is $P(t) = F(t)/A$, where $F(t)$ is the force acting on the fluid over an area A. For the epidural syringe, it was observed that some of the force exerted by the thumb was lost through several factors such as friction, viscosity and off-axis force. Therefore, a coefficient k_a was introduced to account for such losses. Hence, the equation for the static model is

$$P(t) = k_a \frac{F_a(t)}{A} \tag{1}$$

The dynamic model accounts for fluid motion since fluid is continuously injected into the tissue to detect the loss-of-resistance. Given the ratio of the cross-sectional areas of the barrel and needle is approximately 19, and the speed of the plunger is 10 mm/s (far exceeding speeds observed in epidurals), Bernoulli's

equation and the continuity of flow equation for the fluid flowing through two connecting tubes imply the difference in pressure is approximately 20 Pa. The resulting pressure difference is relatively small and not measurable by the instrumentation. Therefore, it was assumed that the pressures from which the fluid flows from the barrel to needle and other cylindrical connections were approximately constant, and the pressure losses from dynamic flow were omitted from modeling.

The decay model includes fluid leakage between the plunger-barrel interface. Two cases were examined: a stationary and a moving plunger. When the plunger was stationary, the pressure, caused by F_a, was observed to decay exponentially from the initial pressure (at the time when the plunger stopped moving). Since the plunger was motionless, small changes in F_a did not affect the initial pressure because it was countered by static friction. If the change in F_a was large, it caused the plunger to move. When the plunger was in motion, pressure did not decay (although some leakage still occurred) because it was continually and directly affected by F_a. Thus, the pressure is expressed as

$$P(t) = \begin{cases} k_a \frac{F_a(t)}{A} & \frac{dD}{dt} \neq 0 \\ k_a \frac{F_a(t_i)}{A} e^{-\frac{t-t_i}{\tau}} & \frac{dD}{dt} = 0 \end{cases} \tag{2}$$

where τ is the exponential time constant and t_i is the time at which the plunger stops moving. A plunger was considered stationary if the speed from the displacement profile was less than 0.18 mm/s which was chosen to be just beyond the noise level of the displacement sensor.

Both k_a and τ were determined empirically in bench tests by measuring the pressure values for a set of constant forces. Thus, k_a was found to be 0.900 ± 0.005 and τ was determined to be 23 ± 8 s. Although a more sophisticated model may be derived, this addressed the main characteristics of the glass syringe that was designed specifically for this low friction application.

2.3 Porcine Study

Epidurals were performed by an experienced anesthesiologist in a manner consistent with clinical practice. The subject was a pig (*Sus scrofa domestica*) that had been culled and prepared according to guidelines for human consumption the same day as the experiments. The hold on the syringe was slightly different to compensate for the instrumentation device, but the loss-of-resistance technique remains unchanged. Ten trials were performed and the punctures took place either between the L2-L3 or L3-L4 vertebrae. During the procedure, an operator monitored the device and acquired the data. When the loss-of-resistance was felt, the anesthesiologist immediately communicated orally to the operator so that the time was recorded. Once the needle breached the epidural space, it was marked at the surface of the puncture and ultrasound (GE Voluson 730 Pro, GE Healthcare, Chalfont St. Giles, Buckinghamshire, UK) was used to image the needle and the epidural space. The software-based ruler was used to measure the puncture path length, the distance between the base of the puncture and

the tip of the needle, in the ultrasound image. A caliper was used to measure the actual puncture path length (the mark to the needle tip). The loss-of-resistance was determined by the times of the minimum slopes of the pressure and displacement measurements. The force profiles nearby the loss-of-resistance tended to vary depending on the anesthesiologist's actions, so the loss-of-resistance was calculated by averaging the time between 90% of the local extrema. The paired student t-test ($\alpha = 0.05$) was used to compare all three times obtained from the force, displacement, and pressure profiles. The mean time of the three estimated times was compared with the time verbally indicated by the anesthesiologist. The physical models (Equations 1 and 2) were used to estimate the pressure from the force and displacement measurements. The mean error and standard deviation between the estimated and actual pressures were calculated. The paired student t-test ($\alpha = 0.05$) was performed on the ten paired depth measurements (ultrasound and actual needle), and the mean and standard deviation were calculated. Just prior to the loss-of-resistance, two regions were also observed (see Section 3) in the displacement profile: a sloped region indicating the needle was in the interspinous ligament and an near-flat region indicating the needle was in the stiffer ligamentum flavum. The mean flow rate, the mean and maximum applied force, the mean and maximum actual pressures, and the mean and maximum calculated pressures were calculated over all trials for each region.

In a second, smaller study, the epidural space depth was *directly* estimated by first manually identifying the epidural space in the ultrasound image without the needle. The depth was then measured vertically to the skin surface (shortest distance) since the needle path was unknown. That depth was compared to a depth *indirectly* determined by estimating the length of the needle tip to the skin surface using the puncture path length and its angle in the ultrasound image. Three trials were performed for each of the L3-L4 and L4-L5 interspaces on a second pig. The mean and standard deviation were used for comparison.

2.4 Human Study

The clinical study was performed on eleven consenting pregnant women who were in labor or prior to Cesarean section.[1] The epidural was performed using the instrumentation device without use of the pressure sensor to avoid contamination. Sterility was maintained by wearing the force sensor under a sterile glove and covering the displacement sensor with a sterile drape prior to mounting it to the sterilized harness attached to the syringe barrel. The needle was initially advanced into the interspinous ligament at either the L2-L3 or L3-L4 interspace. At that time, the data was captured until loss-of-resistance was achieved. Successful delivery of the epidural anesthesia was confirmed by medical assessment of the patient. Measurements of the interspinous ligament and ligamentum flavum regions were performed (except for the actual pressure) over all subjects, as described in Section 2.3.

[1] Approved by the Clinical Review and Ethics Board of the University of British Columbia and B. C. Women's Hospital.

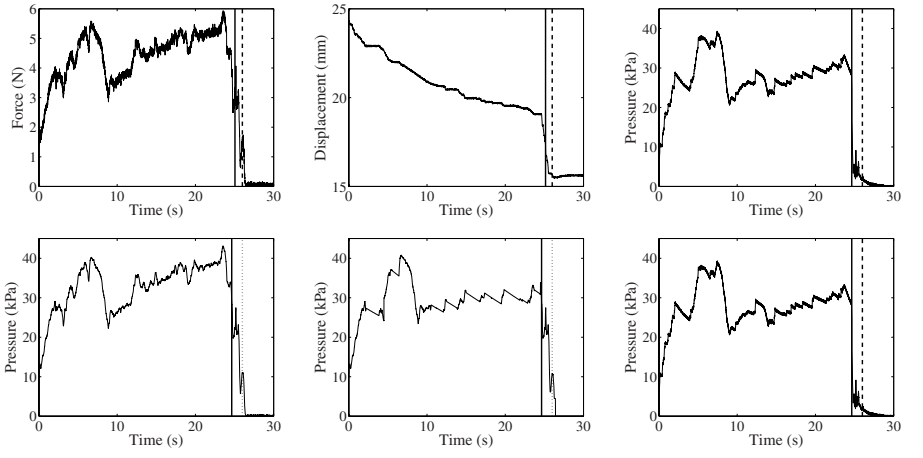

Fig. 2. The top graphs show the applied force, plunger displacement and fluid pressure for a typical epidural procedure. The solid vertical lines indicate the time of loss-of-resistance as determined by each profile (see Section 2.3). The dashed vertical lines indicate the time of loss-of-resistance verbally communicated by the anesthesiologist. The bottom graphs show the estimated pressure from the static, decay model and the measured pressure (which is shown again for the sake of comparison). The solid vertical line for these plots indicates the time of loss-of-resistance determined by the pressure profile.

3 Results and Discussion

3.1 Porcine Study

A typical set of force, displacement and pressure profiles is shown in Figure 2. There are no significant differences between any of the three times of loss-of-resistance estimated from the profiles. Thus, the mean times are calculated and compared with the times verbally indicated by the anesthesiologist. The times indicated by the anesthesiologist are significantly larger, by an average of 0.8 ± 0.3 s, than the mean times. This discrepancy is consistent with the time it takes for the anesthesiologist to conclude entry of the needle into the epidural space and to orally communicate the information to the operator.

The estimated pressures from the static and decay models for the same typical trial are shown in Figure 2. The decay model accounts for leakage with a single time constant (23 s), but the actual pressure profile shows small variations in the decay rate with an average time constant of 22 ± 7 s. Although it is possible that leakage may have occurred in the ligaments, the time constants from the pressure profile and the decay model are nearly the same implying that little or no significant leakage occurs in the dense ligaments for a stationary plunger. For the static model, the average mean error is 2 ± 5 kPa. For the decay model, the average mean error is 0 ± 3 kPa. The decay model is significantly more accurate than the static model, and its standard deviation represents approximately 9%

Table 1. Summary of measurements, averaged over all trials, for the interspinous ligament (ISL) and ligamentum flavum (LF). The calculated pressure values were determined by using the decay model.

Region	Flow Rate (mm^3/s)	F_a (N)	Max F_a (N)	P (kPa)	Max P (kPa)	Calc. P (kPa)	Max Calc. P (kPa)
Porcine - ISL	29 ± 9	2.7 ± 1.6	4.5 ± 1.6	20 ± 10	31 ± 13	20 ± 11	34 ± 13
Porcine - LF	9 ± 7	3.3 ± 1.4	4.1 ± 1.5	27 ± 6	30 ± 7	25 ± 7	32 ± 10
Human - ISL	60 ± 30	2.0 ± 1.4	4.6 ± 1.7	-	-	15 ± 12	35 ± 17
Human - LF	12 ± 13	5 ± 3	6 ± 3	-	-	30 ± 30	40 ± 30

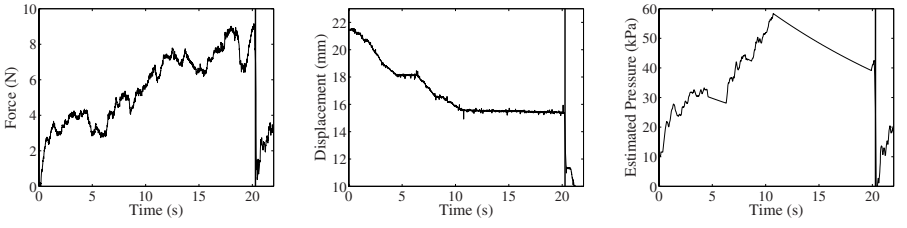

Fig. 3. The graphs show the applied force, plunger displacement and the estimated fluid pressure (based on the decay model) for a typical epidural procedure. The solid vertical lines indicate the time of loss-of-resistance determined by each profile.

that of the peak calculated pressure averaged over all subjects from the clinical study. The measurements for the needle while in the interspinous ligament and ligamentum flavum are summarized in Table 1. We observe low-to-medium forces and measurable plunger movement in the interspinous ligament changing to increasing forces with little plunger movement in the ligamentum flavum followed by a rapid fall upon entry into the epidural space.

Ultrasound was used to image the needle once it had entered the epidural space. The mean error of the puncture path length is 0.0 ± 0.5 mm. There is no significant difference between the two measurements confirming that the ultrasound measurements are consistent with the actual measurements when the needle itself was visible in the ultrasound. The depiction of the epidural space is characterized by a "doublet", a horizontal line pair of the interface between the ligamentum flavum and epidural space. In the second study, the average direct and indirect measurements of the epidural space depth for the L3-L4 interspace are 29.5 ± 0.8 mm and 29 ± 2 mm, respectively, and for the L4-L5 interspace are 35.7 ± 1.7 mm and 37 ± 4 mm, respectively. We conclude the direct and indirect measurements are consistent with the instrumented loss-of-resistance technique.

3.2 Human Study

In the clinical study, a typical trial is shown in Figure 3. The measurements for the needle while in the either the interspinous ligament or ligamentum flavum are summarized in Table 1. Although there is large patient variability, the profiles and ligament properties are similar to the ones from the porcine study

(see Section 3.1). Additionally, human interspinous ligament and ligamentum flavum are less amenable to saline injection in the human spine in vivo than those of the porcine spine in vitro.

4 Conclusion

A low-cost, sterilizable and unobtrusive instrumentation device for the loss-of-resistance was developed for both porcine and human subjects. The loss-of-resistance is easily visible and consistent among the force, displacement and pressure profiles, and the oral indication by the anesthesiologist. Furthermore, the location of the epidural space detected by the loss-of-resistance is validated using ultrasound measurements. The decay model relating the pressure to the applied force and plunger displacement has a standard deviation of approximately 9% that of the peak calculated pressure in the clinical study. When the plunger was stationary, there was negligible leakage into the interspinous ligament and ligamentum flavum. The measurements also show the ligamentum flavum is generally less amenable to saline injection than the interspinous ligament. The instrumentation of loss-of-resistance will allow further study into tissue properties, patient variability, and operator performance.

References

1. Le Coq, G., Ducot, B., Benhamou, D.: Risk factors of inadequate pain relief during epidural analgesia for labour and delivery. Can. J. Anaesth. 45, 719–723 (1998)
2. Watts, R.W.: A five-year prospective analysis of the efficacy, safety, and morbidity of epidural anaesthesia performed by a general practitioner anaesthetist in an isolated rural hospital. Anaesth. Intensive Care 20(3), 348–353 (1992)
3. Grau, T., Bartusseck, E., Conradi, R., Martin, E., Motsch, J.: Ultrasound imaging improves learning curves in obstetric epidural anesthesia: a preliminary study. Can. J. Anaesth. 50, 1047–1050 (2003)
4. Konrad, C., Schupfer, G., Wietlisbach, M., Gerber, H.: Learning manual skills in anesthesiology: Is there a recommended number of cases for anesthetic procedures? Anesth. Analg. 86, 635–639 (1998)
5. Magill, J., Anderson, B., Anderson, G., Hess, P., Pratt, S.: Multi-axis mechanical simulator for epidural needle insertion. In: Cotin, S., Metaxas, D.N. (eds.) ISMS 2004. LNCS, vol. 3078, pp. 267–276. Springer, Heidelberg (2004)
6. Dang, T., Annaswamy, T.M., Srinivasan, M.A.: Development and evaluation of an epidural injection simulator with force feedback for medical training. Stud. Health Technol. Inform. 81, 97–102 (2001)
7. Carden, E., Ori, A.: The bip test: a modified loss of resistance technique for confirming epidural needle placement. Pain Physician 9(4), 323–325 (2006)
8. Marhofer, P., Willschke, H., Greher, M., Kapral, S.: New perspectives in regional anesthesia: the use of ultrasound - past, present, and future. Can. J. Anaesth. 52(6), R1–R5 (2005)